Wind Energ. Sci., 11, 1791–1802, 2026
https://doi.org/10.5194/wes-11-1791-2026

eawe european academy of wind energy
Open Access WIND ENERGY SCIENCE

Uniform blade pitch misalignment in wind turbines: a learning-based detection and classification approach

Sabrina Milani[1], Jessica Leoni[1], Stefano Cacciola[2], Alessandro Croce[2], and Mara Tanelli[1]

[1]Dipartimento di Elettronica, Informazione e Bioingegneria (DEIB), Politecnico di Milano, Piazza L. Da Vinci 32, Milan, 20133, Italy
[2]Dipartimento di Scienze e Tecnologie Aerospaziali (DAER), Politecnico di Milano, Politecnico di Milano, Via La Masa, 34, Milan 20156, Italy

Correspondence: Sabrina Milani (sabrina.milani@polimi.it), Jessica Leoni (jessica.leoni@polimi.it), Stefano Cacciola (stefano.cacciola@polimi.it), Alessandro Croce (alessandro.croce@polimi.it), and Mara Tanelli (mara.tanelli@polimi.it)

Received: 12 August 2025 – Discussion started: 1 September 2025
Revised: 22 February 2026 – Accepted: 12 April 2026 – Published: 20 May 2026

Abstract. Maintaining wind turbines in efficient and optimal working conditions is crucial to maximize energy production and reduce unexpected downtime, especially in remote or offshore installations. Pitch misalignment is one of the most common issues affecting wind turbine performance. Our previous studies addressed the automatic detection of such a fault using signals from mechanical moments collected from the fixed and rotating reference frames. Specifically, the introduced approaches involve applying machine learning techniques to ad-hoc-designed physics-based indicators, extracted from the mentioned signals, to detect the misalignment and localize the fault. Despite the fact that these approaches work effectively in the case of both single and multiple blades misaligned simultaneously, conditions in which all blades are misaligned by the same quantity have not been taken into account. Unlike individual blade misalignments, this fault presents unique challenges in its detection due to the symmetrical nature of the fault, which minimizes immediate operational disruptions but gradually impacts turbine performance and energy efficiency. To also account for this condition, in this paper, we present an innovative methodology to identify and classify uniform pitch misalignment across all wind turbine blades. This issue has been scarcely explored in existing literature, leaving a critical gap in the understanding and diagnosis of uniform pitch misalignment. Extensive results conducted with linear and turbulent wind conditions prove the effectiveness of our approach at identifying and quantifying the entity of the misalignment, thus paving the way for more efficient and reliable wind turbine diagnostics.

1 Introduction

Persistent vibrations caused by aerodynamic imbalances in wind turbines can have a critical impact on the power production efficiency and mechanical health of these systems, potentially leading to failures in essential components as electronics, sensors, gearboxes, and blades. These issues often lead to reduced energy production and require frequent maintenance inspections, which can be costly and challenging. Therefore, research has been conducted to design automatic systems to promote the transition from time-based to condition-based maintenance scheduling, leading to savings and reducing downtimes.

1.1 Related works

Proactive monitoring and fault detection in wind turbines have been widely investigated in the literature, motivated by the need to increase system reliability, reduce operation and maintenance costs, and enable condition-based maintenance strategies. Both physics-based and data-driven approaches have been proposed and applied to different turbine subsystems, including drivetrain, generator, control, and pitch sys-

tems, often leveraging SCADA data and machine learning techniques (Zaher et al., 2009; Tautz-Weinert and Watson, 2017; Stetco et al., 2019; Al Lahham et al., 2024). Among the several issues, pitch misalignment in wind turbines is one of the most common and severe. This issue has been traditionally studied using two main approaches: physics-based methods and machine learning techniques. Physics-based methods, as explored in works such as Dalsgaard et al. (2009) and Cacciola et al. (2016), rely on physical models of the system to identify anomalies like rotor imbalances. Other model-based approaches, discussed in Desheng et al. (2021), Cacciola et al. (2018), Bertelè et al. (2018), and Cacciola and Riboldi (2017), aim to address rotor imbalances by employing load compensation or control strategies. All these methods provide a detailed understanding of system dynamics, but they often require a highly specific model tailored to the turbine, limiting their adaptability to different real systems. Moreover, some of the approaches depend on signals that might be difficult to measure in real-world scenarios, limiting large-scale adoption. Last, they frequently struggle with accuracy and reliability in turbulent wind conditions, which are typical during wind turbine operations.

On the other hand, machine learning approaches, such as those presented in Kusiak and Verma (2011) or those presented in Cacciola et al. (2016), which include deep learning models, provide a more flexible and efficient framework. Examples range from classical data-driven techniques (Kusiak and Verma, 2011) to more advanced frameworks specifically targeting pitch system monitoring and fault detection (Yang et al., 2018; Li and Wang, 2019; Tang et al., 2021; Qin et al., 2023). Despite their generality, these methods often lack interpretability, which may represent a drawback in industrial applications due to certification requirements and the need for actionable insights during maintenance interventions. Furthermore, they may face challenges in accurately localizing anomalies or quantifying their severity.

In our earlier works (Milani et al., 2024, 2025), to overcome the limitations and combine the strengths of both approaches, we introduced a novel framework leveraging interpretable physics-based features extracted from mechanical moment signals. This approach effectively detects, classifies, and localizes pitch misalignment, focusing on cases where one or multiple blades are misaligned simultaneously. Specifically, feature extraction is performed in real time using physics-based frequency- and time-domain features computed over a fixed number of rotor revolutions, thus avoiding dependency on rotor speed. The framework is divided into two stages: the first layer detects the presence of pitch misalignment and classifies the fault severity, while the second layer localizes the affected blade(s). Although the framework shows satisfactory performance even under turbulent wind conditions, the scenario in which all blades are uniformly misaligned has not been considered in our previous studies. Moreover, to the best of the authors' knowledge, this scenario has received limited attention in the existing literature. Indeed, it represents a particularly challenging case due to the symmetrical nature of the fault, which complicates detection. Pitch fine-tuning and performance coefficient optimization have historically been addressed within the wind turbine control literature, where the objective is to maximize energy capture rather than to explicitly identify faults or offsets. In this context, extremum seeking control (ESC) has been widely investigated as a model-free optimization strategy for online Cp–λ optimization, with applications to wind turbine pitch control (Krstić and Wang, 2000; Rotea, 2000; Bodson et al., 2014). Experimental validation of ESC-based controllers on real wind turbines has also been reported, demonstrating their practical feasibility (Johnson et al., 2016). However, such control-oriented approaches aim at compensating for performance losses and may therefore mask the presence of underlying pitch offsets, whereas the present work explicitly targets their detection within a proactive monitoring framework. Identifying this fault is critical, as the turbine may not exhibit an immediate reduction in power production, further concealing the anomaly while potentially causing long-term degradation of mechanical components.

Detecting situations where all blades are uniformly misaligned is practically relevant. Consider the most general case where the three blades have generic pitch offsets $\Delta\beta_1$, $\Delta\beta_2$, and $\Delta\beta_3$, collected in the vector $\boldsymbol{p} = \Delta\beta_1,\ \Delta\beta_2,\ \Delta\beta_3^T$. Any pitch configuration can be decomposed into two parts:

- a *uniform misalignment*, defined as $\Delta\beta_u = \frac{\Delta\beta_1+\Delta\beta_2+\Delta\beta_3}{3}$, which is common to all blades and produces no aerodynamic imbalance, and
- a *residual misalignment* $\boldsymbol{p}_{res}$ with zero mean, responsible for the aerodynamic imbalance.

This decomposition is unique: each physical misalignment $\boldsymbol{p}$ corresponds to exactly one pair $(\Delta\beta_u, \boldsymbol{p}_{res})$ and vice versa. Therefore, if uniform misalignment is not observable, the three pitch offsets can only be determined up to an unknown constant offset, limiting the detection of the most general form of aerodynamic imbalance.

1.2 Problem statement

As previously mentioned, in the particular case in which all the blades are uniformly misaligned, the fault has a symmetrical nature. This means that loads and vibrations are evenly distributed on the blades and the tower of the turbine. This particular symmetrical behavior can mask the typical symptoms of misalignment, making it more similar to a nominal behavior. As a consequence, it becomes harder for traditional diagnostic methods to detect the fault: indeed, the previous architecture would classify these cases as healthy and non-anomalous ones. To tackle this issue, in this work we aim at identifying this condition by not considering vibrational behavior only or power production by moving the focus to the entity of the control action. In fact, collective

pitch control has a pivotal role in wind turbine systems as it regulates power output production and ensures optimal operational efficiency. The collective pitch system modulates the pitch blade angles of all blades to ensure that the wind turbine operates at its rated power output, in power region III, namely, above the rated wind speed. Whenever a uniform pitch misalignment is present, the regulator might demand unusual collective pitch adjustments to compensate for the altered aerodynamic behavior to maintain a balance between aerodynamic forces and generator demands. On the other hand, below the rated speed (i.e., in power region II), the system functions in a working regime where the blades pitch is kept constant and the power output is regulated through torque variations. For this reason, the analysis focuses on two distinct wind regimes, and it is designed to be effective not only in ideal wind conditions, but also in turbulent and more realistic scenarios. In Fig. 1 the scheme of the overall hierarchical architecture is presented with an additional layer dedicated to the detection of uniform misalignment.

Accordingly, if non-symmetrical misalignment is detected, then the previous presented methodology is applied so that the fault is classified according to its severity and localized on the related blades by considering features related to the mechanical moment features. On the other hand, if a healthy case is detected, an additional verification step needs to be performed. In fact, as previously mentioned, given the symmetrical characteristics of the fault, uniform misalignments could be mistakenly identified as healthy cases by previous approaches. Therefore, this new introduced layer is devoted to further checking the supposed healthy cases to identify eventual uniform misalignment conditions. In the latter case, the degree of the misalignment is precisely quantified based on the behavior of the control action in power region III or by assessing mechanical moments within the blades' reference frame in power region II.

2 Methods

The dataset consists of several 600 s simulations, sampled at 5 Hz, generated by a virtual model of a reference 5 MW wind turbine (Jonkman et al., 2009) implemented in the software `Cp-Lambda` (Code for Performance, Loads, Aeroelasticity by Multi-Body Dynamic Analysis), a state-of-the-art general-purpose multibody simulator (Bottasso and Croce, 2009–2018). The model of the turbine is characterized by a flexible tower, blades, and shaft, whereas blade element momentum theory is used for modeling rotor aerodynamics, including hub and tip losses and tower shadow. To measure relevant signals, the turbine model is also equipped with virtual sensors, and all simulations were conducted in different pitch misalignment conditions, uniformly imposed on the three blades. Moreover, two scenarios have been considered, including turbulent inflow that was defined according to the IEC standards (IEC requirements book Wind Turbines, 2004) (Normal Turbulence Model, NTM) and leveraging numerical weather prediction (NWP), considering Turbulence C. According to the IEC standard, this class corresponds to a reference turbulence intensity $I_{\mathrm{ref}} = 0.12$, representing relatively low ambient turbulence conditions. The turbulence intensity varies with the mean wind speed following the IEC prescription and is typically associated with low-roughness or offshore sites. Multiple turbulence realizations were considered by varying the turbulence seed in order to ensure statistical robustness. In addition, the simulations are conducted with an air density set at $\rho = 1.225\,\mathrm{kg\,m^{-3}}$ and wind speeds ranging from $v = 5\,\mathrm{m\,s^{-1}}$ to $v = 25\,\mathrm{m\,s^{-1}}$, with the wind direction aligned with respect to the rotor, meaning with zero-mean yaw misalignment. The full list of simulations (from cut-in to cut-out speed) was repeated 22 times, with different uniform pitch misalignment values, and the turbulence seed for NTM cases was changed every time. In Table 1, an overview of the key characteristics of the conducted simulations is summarized, including information on air density, turbulence level, and wind speed.

Table 1. Simulation parameters.

Simulation setting	Value
Air density	$\rho = 1.225\,\mathrm{kg\,m^{-3}}$
Turbulence type	NTM – NWP
Turbulence class	C – [–]
Wind speed range	$v = 5:25\,\mathrm{m\,s^{-1}}$
Mean yaw misalignment	0°

In particular, 16 sets of simulations were dedicated to all uniformly misaligned blades and 6 sets for the balanced scenario, i.e., without misalignment. The maximum entity for the considered pitch offset is $\pm 2.0°$, while the minimum one is equal to $\pm 0.5°$.

2.1 Exploratory analysis and feature engineering

The general idea is to compare the behavior of the system in healthy and uniform scenarios and then derive a comprehensive physical understanding of the key differences to define the set of relevant signals from which to extract features to quantify the fault when present.

2.1.1 Signal processing

According to the physical knowledge of the system, in a balanced rotor, loads are transmitted to the fixed frame at harmonics that are multiples of the number N_{B} of blades only (in the case under study, $N_{\mathrm{B}} = 3$). Conversely, unbalanced rotors transmit loads at all harmonics, with the $1\times$ Rev frequency being the most evident one.

Therefore, in our previous studies (Milani et al., 2024, 2025), the major indicators highlighting the existence of the once-per-revolution $1\times$ Rev harmonic component as-

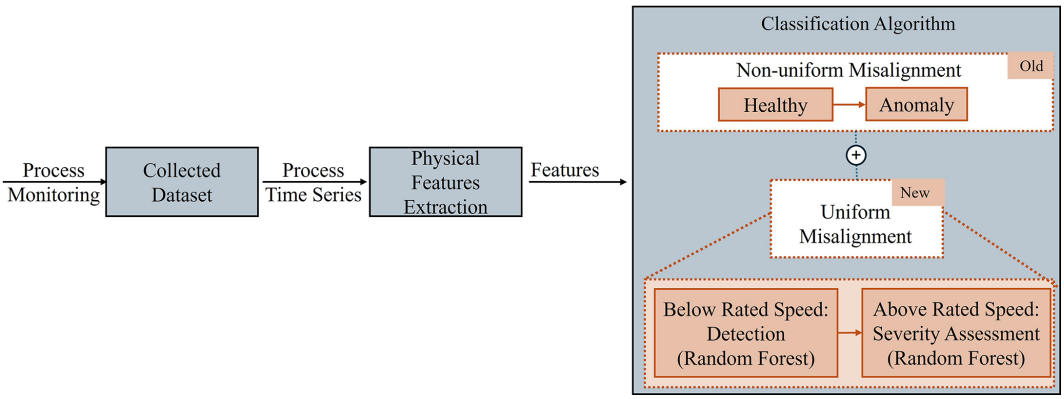

Figure 1. Hierarchical detection and localization architecture.

sociated with the rotor rotational speed in a non-uniform misaligned scenario were the mechanical moments along the lateral and vertical axes. Yet, when all the blades are uniformly misaligned, loads are still transmitted to the fixed frame at harmonics that are multiples of the number N_B of blades only, without showing the $1\times$ Rev frequency component. Therefore, from this first analysis, a healthy case or a uniform misaligned case would be challenging to distinguish as they behave similarly. Thus, according to our previous approaches, a uniform misaligned case would be detected as healthy.

Figure 2 illustrates azimuth-based power spectra at a medium wind speed of $v = 15\,\mathrm{m\,s^{-1}}$ for the yawing moment along the z direction in a healthy case and different anomalous cases (from ± 0.5 and $\pm 2.0°$ misalignment in either NTM or NWP scenarios). As in the previous studies, to avoid dependency on the wind speeds, the Fourier transformations applied on the signals are performed with respect to the azimuth signal, rather than to time. In such a way, the harmonic response depends on the rotor frequency revolutions only. As previously mentioned, all cases *do not* exhibit a peak placed around the $1\times$ Rev harmonic irrespective of the turbulence condition or the wind speeds.

It is evident that, from the traditional analysis based on the presence of the peak at the $1\times$ Rev performed on the spectra, healthy and anomalous cases cannot be easily distinguished. Therefore, further investigation of additional signal behaviors is necessary. One way to investigate the presence of the fault could be the analysis of the output power production, which indeed may lead to worthless insights, as these systems are controlled by a pitch regulator especially at high wind speeds. Figure 3 shows the power curve in a healthy and faulty case for different wind speeds. As reported in the figure, due to the controller action, especially at high wind speeds, the power curves in a healthy and faulty case are not distinguishable. On the other hand, we rely on the domain knowledge that whenever multiple blades are affected by pitch misalignment, there may be a noticeable impact on collective pitch demand from the control system. Thus, we investigate if this deviation in the regulator's collective pitch signal can provide a supplementary indicator for detecting and classifying the misalignment.

As expected, we noticed that the pitch adjustments required by the controller in the misaligned cases might be relevant when compared with the healthy cases and reveal patterns that are distinct from a healthy rotor. Therefore, some relevant features can be extracted for this signal, such as the mean pitch angle, variance, and the difference in the absolute value of the collective demanded pitch with respect to a healthy case. Additionally, power production might be informative at least until the control action reaches a steady state. On the other hand, for wind speeds below the rated value, the pitch controller is not active, as the torque control is responsible for regulating the turbine's operation. Thus, control-action-related features are not useful in this region, but mechanical moments measured along the y and z directions on the local reference frame of the blades turned out to be effective as they exhibit noticeable deviations when compared to a healthy baseline in the time domain, making them valuable indicators of the analysis in this region.

2.1.2 Feature extraction

In our previous research, we outlined the need for an interpretable machine learning framework for the detection and classification architecture for both certification and adoption purposes. Thus, we take interpretability into account in the whole design of the presented framework. To this end, we focused solely on extracting physics-based features, which would lead to a better understanding of the decision-making process adopted by the classifier. Moreover, we choose to rely on an interpretable machine learning technique, i.e., random forest, which is capable of explaining its decision-making process to the domain expert. According to the preliminary analysis results, given that $1\times$ Rev harmonics and the power curve do not play a crucial role in detecting the presence of the anomaly, we have focused on extracting features related to the collective demanded pitch and the me-

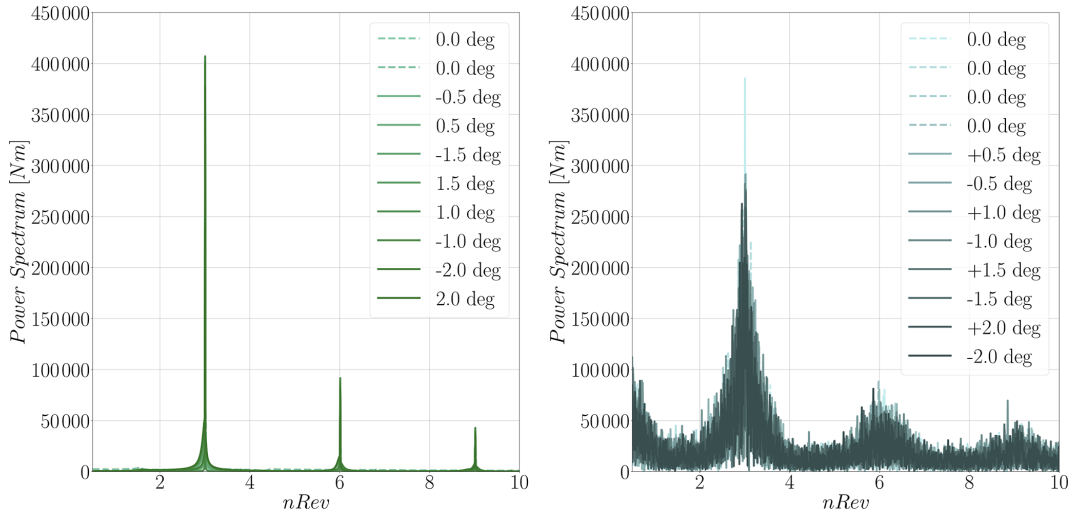

Figure 2. Mechanical moment spectra for healthy and different misaligned cases for NWP (on the left) and NTM scenarios (on the right), all at a wind speed of 15 m s^{-1}.

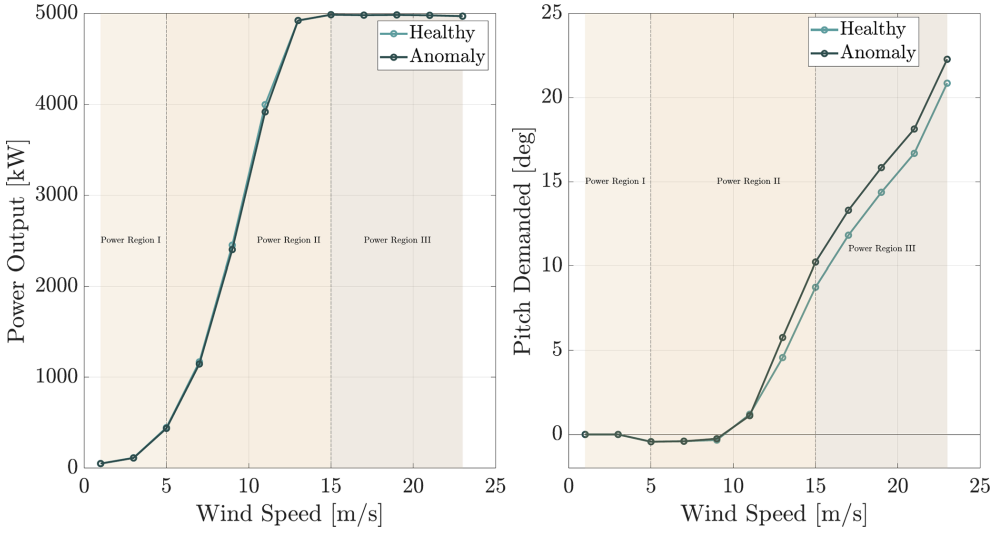

Figure 3. Mean power and pitch curves in two different cases: healthy and anomalous −1.5°.

chanical moments on the blades in the time domain. Specifically for wind speed higher than the rated speed, we extracted the following:

- M_{p} – mean value in a specified time interval of the collective demanded pitch
- σ_{p} – standard deviation value in a time interval of the collective demanded pitch
- Δ_{p} – the absolute value of the difference between the mean collective demanded pitch in a healthy scenario and the considered scenario $\Delta_{\mathrm{p}} = |M_{\mathrm{p,healthy}} - M_{\mathrm{p,case}}|$ (in this case, null values are expected when the current considered case is a healthy scenario, while a difference linearly dependent on the severity of the misalignment is expected when considering an anomalous case).

On the other hand, for wind speed lower than the rated speed, we rely on the mechanical moments along the y and z directions, and we extracted the following:

- M_{yi} and M_{zi} – the mean value in a specified time interval of the mechanical moments along y and z on the ith blade (where $i = 1, 2, 3$)
- Δ_{M_y} and Δ_{M_z} – the absolute value of the difference between the mean mechanical moments along y or z in a healthy scenario and the considered scenario $\Delta_{My} = |\sum_{i=1}^{3} M_{y,i} - \sum_{i=1}^{3} M_{y,i}^{\mathrm{H}}|$ and $\Delta_{M_z} = |\sum_{i=1}^{3} M_{z,i} - \sum_{i=1}^{3} M_{z,i}^{\mathrm{H}}|$, respectively.

These time-domain features are extracted using a moving-window approach, as in the original framework, to ensure that the classification algorithm's predictions are generated in real time. As it is known in the literature, the size of the window plays a prominent role in determining the performance of the detection approach. Thus, we conduct a tailored sensitivity analysis to find the optimal length, as described in Sect. 2.2.

2.2 Detection and severity assessment

After feature extraction is completed, depending on the operational conditions dictated by the wind speed, two distinct methods are applied. If the working condition is referring to a wind speed lower than the rated speed (i.e., power region II), then the focus is on the mechanical moments on the blade, and the coordinates of each feature point are determined by Δ_{My} and Δ_{Mz}. In this case, each extracted window corresponds to a point in a 2D space. Conversely, when the wind speed is above the rated speed, then the coordinates of each feature point are determined by the mean or standard deviation of the collective demanded pitch and the difference with respect to a healthy case. Thus, each window corresponds to a point in a 3D space. All these instances derived from this process are exploited for training and evaluating the performance of two different *random forest classifiers*. These classifiers are capable of distinguishing the presence of misalignment from a healthy case and in the case of a uniformly misaligned rotor by quantifying the severity of the misalignment located on all the blades in power region III. As previously mentioned, the random forest algorithm has been selected for its interpretability and robustness, as it is one of the most explainable state-of-the-art bagged tree-based classification methods (Breiman, 2001). This approach combines the outcomes of numerous binary decision trees, which iteratively split the data to reduce variations within the identified nodes at each step. The splitting process is carried out considering specific criteria, including accuracy, precision, and the Gini index (Ceriani and Verme, 2012). This last metric can also be considered to interpret the classifier logic by quantifying the relevance of each feature in contributing to classifying the instances. In particular, each classifier (for low and high speeds) was trained on the related instances to recognize the presence of misalignment from the features of interest in that speed condition. The classifier for lower wind speeds is binary, while the other recognizes five conditions, namely 0° for healthy cases and the following misalignment degrees for misaligned cases: ± 0.5, ± 1.0, ± 1.5, and $\pm 2.0°$. Both classifiers also work in NTM and NWP conditions. Last, it is important to note that in designing the architecture, the proper fine-tuning of two sets of hyperparameters was key, which were the window size for feature extraction and the classifiers' depth and number of estimators. We adopted a trade-off between accuracy and computational time, which increases with the depth of each instance of a tree.

Table 2. Definition of evaluation metrics.

Metric	Definition
Precision	TP/(TP+FP)
Recall	TP/(TP+FN)
F1 score	2TP/(2TP+FP+FN)

Data are split according to a balanced fashion into 70.0 % for training and 30.0 % for testing in a stratified manner; additionally, 10-fold cross-validation is applied, and the average performance across all folds is reported. Evaluation metrics, including precision, recall, and F1 score, were chosen for their relevance in evaluating the performance of anomaly detection methods. Precision measures the accuracy of predictions by evaluating the proportion of correctly predicted instances to the total predicted instances for a specific class. In contrast, recall assesses the accuracy of predictions for a class relative to all actual instances of that class. The F1 score provides a balanced measure by combining both precision and recall, representing their harmonic mean, as reported in more detail in Table 2. Lastly, support represents the number of occurrences of each label within the analyzed class.

3 Results and discussion

This section reports and discusses the results obtained in the extensive validation of the approach. As reported in Sect. 1, a main contribution of this work is to address uniformly distributed misalignment not only in stationary wind conditions but also in turbulent wind conditions. Therefore, we present the results achieved in both stationary and turbulent wind conditions. Fine-tuning of the parameters shows that the second scenario is more challenging, yet optimal performance can still be achieved.

3.1 NWP data

We first evaluate the method considering ideal NWP cases in which no turbulence is considered, and therefore no noise on the signals is present. In this scenario, the classification and detection procedures prove to be highly effective and accurate.

3.1.1 Region II – below rated speed

First, the scenario in which the wind speed is below the rated wind speed, $V = 13\,\mathrm{m\,s^{-1}}$, is considered. As reported in Sect. 2.2, the RF classifier dedicated to low speeds performs binary classification (healthy vs. uniform). Therefore, Δ_{My} and Δ_{Mz} features are taken into account. As previously mentioned, the moving-window length has been carefully chosen to balance resolution on the signals and computational efficiency, and a window of 4.3 min is chosen in this case as the minimum value that leads to reaching an F1

Table 3. Metrics computed from the fault detection output considering NWP cases.

Classification report				
Label	Precision	Recall	F1 score	Support
Healthy	0.99	0.99	0.99	24
Misaligned	0.98	0.98	0.98	92

Table 4. Metrics computed from the fault detection and quantification output considering NWP cases.

Classification report				
Label	Precision	Recall	F1 score	Support
Healthy	1.00	0.89	1.00	24
0.5°	1.00	1.00	1.00	23
1.0°	0.92	1.00	0.96	22
1.5°	0.95	0.95	0.95	19
2.0°	1.00	0.93	0.96	28

score of 99.15 % in detecting the presence of the anomaly with a wind speed ranging from 5 to 11 m s^{-1}. In this specific case, the hyperparameter of the model includes a number of estimators equal to 2 with a depth of 5. To provide further insights into the classification outcomes, Fig. 4 provides a graphical representation of the results, showing the actual and estimated instances for each predicted window along with the corresponding confusion matrix. In the plot, each point corresponds to a window, and its coordinates are Δ_{My} and Δ_{Mz}. As demonstrated in the figure, instances are graphically well separable and show a linear trend, allowing the classifier to achieve high classification performance.

Table 3 shows fault detection metrics considering NWP cases.

3.1.2 Region III – above rated speed

When the wind speed is above the rated speed, we rely on the demanded collective pitch, and, on the other hand, further classification of the severity of the misalignment can be performed. Average results for evaluation metrics, including precision, recall, F1 score, and support for this scenario, are reported in Table 4. By considering the F1 score as a metric, our approach proved to be effective at not only detecting the presence of a uniform misalignment but also further classifying its severity class, with an average F1 score of 97.41 % after a 4.3 min interval and with a wind speed ranging from 13 to 25 m s^{-1}. Here, the model architecture is slightly more complex, comprising a total of five estimators, each with a depth of 20.

More specifically, our framework exhibits an excellent F1 score, achieving 100.0 % accuracy in detecting the healthy class, 100.0 % for the 0.5° class, 96.0 % for the 1.0 and 2.0° classes, and 95.0 % for the 1.5° class. Indeed, these achievements stand out as remarkable, since starting from a wind speed of $v = 13$ m s^{-1}, the algorithm is capable not only of detecting the presence of a uniform misalignment but also of precisely assessing its severity. To provide further insights into the classification outcomes, Fig. 5a and b provide a graphical representation of the results, showing the actual and the estimated severity degree for each predicted window. In the plot, each point corresponds to a window, and its coordinates are the mean demanded collective pitch and the delta pitch with respect to a healthy case. It can be seen that, due to the effective feature engineering, the different misalignment conditions are well separated, easing the classification task. Indeed, predicted points consistently overlap with actual ones, especially for the healthy cases. Indeed, given that the system in this scenario is not affected by noise, Δ_p values are strictly set to 0, leading to excellent detection capabilities. Also, it can be seen that the prediction of the model indicates a strong correspondence between the real and predicted system behavior, with small variance with respect to the actual misalignment degree.

3.2 NTM data

As previously mentioned, more challenging but more likely operating conditions are still considered in our work, including turbulent scenarios and strong winds. The only limitation is on the minimum wind speed, which increases from 13 to 15 m s^{-1} for a more precise misalignment quantification. This is due to the fact that the machine operates across two different power regions, separated by the rated speed as previously mentioned. Given the more turbulent scenario and the presence of noise, distinguishing between the two regions becomes more challenging. Consequently, higher wind speeds are required to clearly identify the operating region and observe the corresponding pitch changes.

3.2.1 Region II – below rated speed

As previously done in the stationary case, for a lower wind speed range, the mechanical moments on the blades can be exploited for the anomaly detection. In this case, a 10 min window length is required for reliable detection. Again, Fig. 6 depicts the actual and predicted instances for a wind speed ranging from $v = 5$ m s^{-1} to $v = 13$ m s^{-1} with an F1 score of 94.1 % when considering a model architecture composed of 20 trees with a depth of 5.

3.2.2 Region III – above rated speed

Conversely, when considering wind speeds higher than the rated speed $v = 15$ m s^{-1}, different scenarios can be explored. We first tried to keep the same window size of the stationary case, namely the short 4.3 min interval. However, in power region III, this window length only allows for ac-

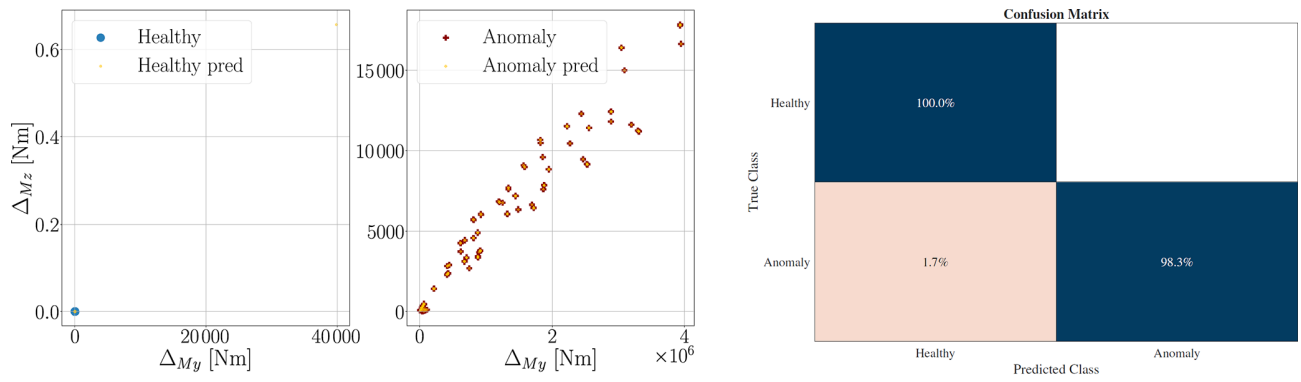

(a) (b)

Figure 4. Misalignment detection assessment results. **(a)** Prediction timeline showing healthy and anomalous cases (yellow) compared with ground truth. Feature comparison between predicted and actual classes. **(b)** Confusion matrix of the misalignment detection model. Confusion matrix summarizing classification performance.

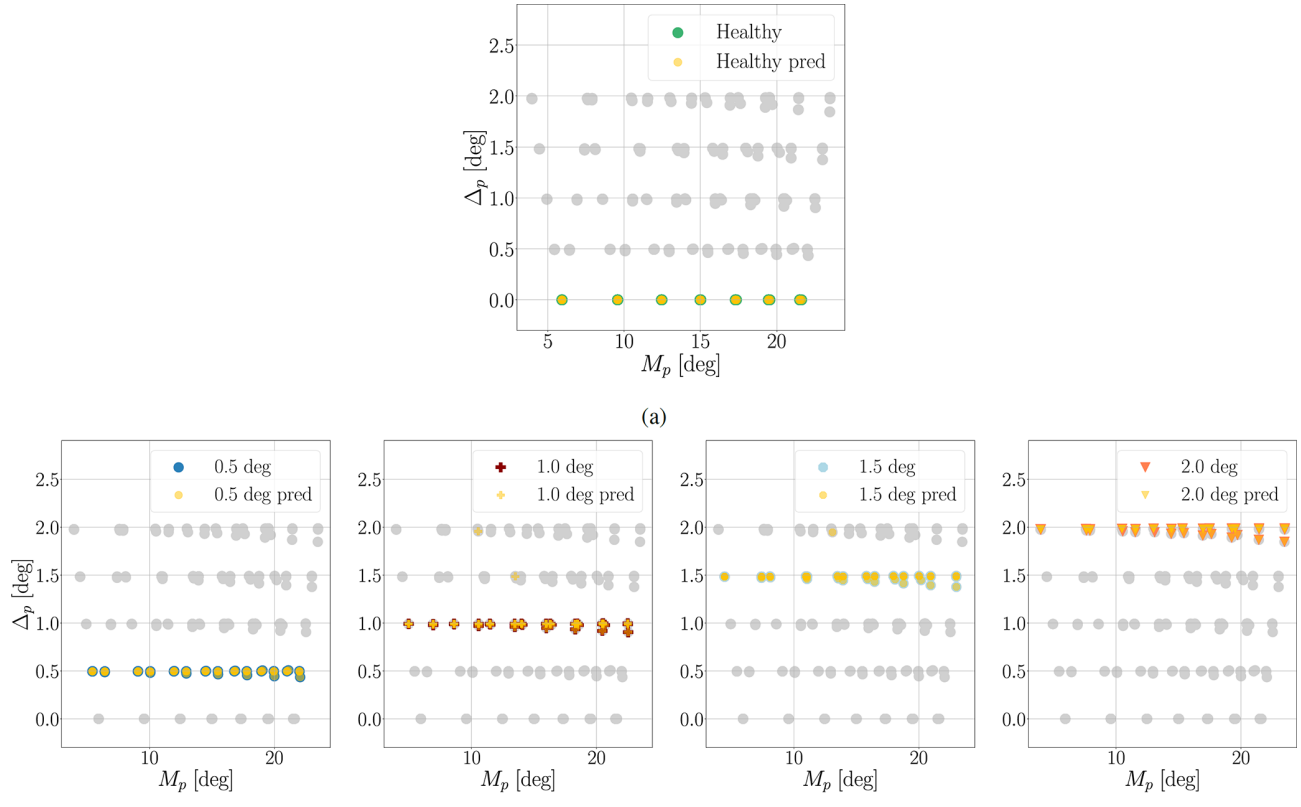

(a)

(b)

Figure 5. Misalignment severity assessment results. **(a)** Healthy cases. Predicted healthy cases (yellow) compared with the actual severity levels. **(b)** Misalignment severity. Predicted anomaly cases (yellow) compared with the actual severity levels.

curate detection of the presence of a uniform misalignment, without enabling a precise quantification of its severity. To achieve such a detailed assessment of the misalignment for higher wind speeds, a larger time window is required. This highlights a trade-off between speed and precision: a rapid response enables only binary detection, whereas a more accurate evaluation of the misalignment severity demands a longer time frame. Given that this specific anomaly evolves over time, and in view of practical applications, a 10 min window is recommended. This choice also allows the use of the two adopted models developed in the ideal scenario. To begin with, the results for the evaluation metrics, includ-

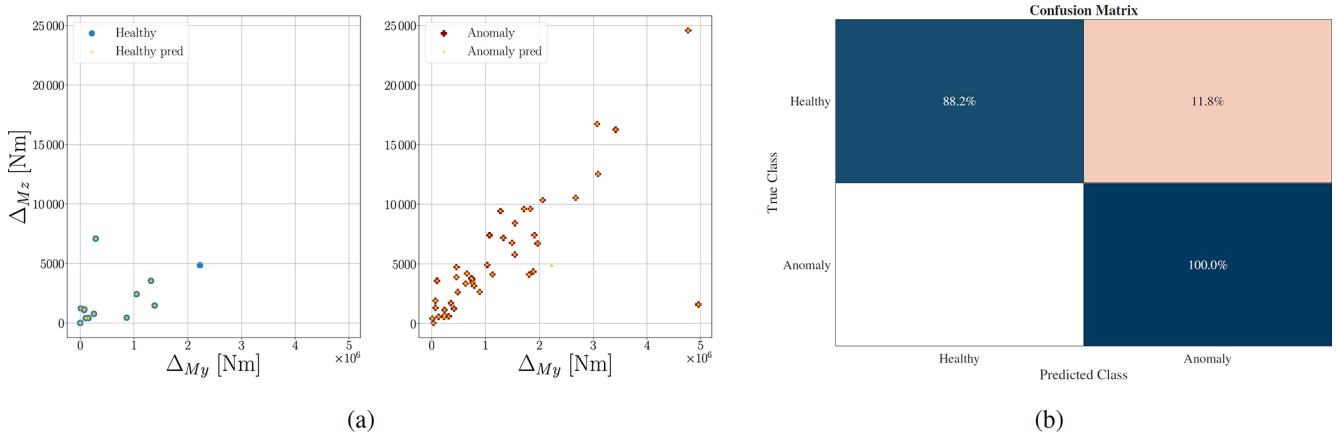

(a) (b)

Figure 6. Misalignment detection assessment results for the NTM configuration. **(a)** Prediction timeline showing healthy and anomalous cases (yellow) compared with ground truth. Feature comparison between predicted and actual classes. **(b)** Confusion matrix of the misalignment detection model. Confusion matrix summarizing classification performance.

ing precision, recall, F1 score, and support, are reported in Table 5 for the detection performance within the short time window of 4.3 min. Using the F1 score as a reference metric, our approach proved effective at detecting the presence of a uniform misalignment, with a promising average F1 score of 91.5 %. This result, while slightly lower than in the case of linear wind conditions, still confirms the method's effectiveness in power region III. As previously mentioned, the wind speed in this scenario ranges from 15 to 25 m s^{-1}. A sensitivity analysis has been carried out by considering different window lengths, and the performance metrics for different window sizes inherently increase by increasing the windows size. In Fig. 7a, the F1 score performance is reported when considering three different moving windows. When considering a larger time window, detection performance increases, and this leads us to consider a larger time window of 10 min for the classification. Thus, with a longer time window, as anticipated, not only can the misalignment detection be performed, but a more precise quantification of the entity of the fault can be performed as well.

Figure 7b provides a graphical representation of these binary detection results, showing the actual and estimated misalignment for each predicted window. As before, in the plot, each point corresponds to a window, and its coordinates are the mean demanded collective pitch and the delta pitch with respect to a healthy case. As demonstrated in the figure, the data are accurately classified despite being more spread in the space.

When extending the time window to 10 min, a more accurate assessment of the misalignment severity also becomes possible. In Table 6, the metrics for the quantification procedure performance are reported.

Indeed, these achievements stand out as remarkable, since starting from a wind speed of $v = 13$ m s^{-1}, the algorithm is capable of not only detecting the presence of a uniform misalignment but also precisely assessing its severity with an average F1 score of 96.82 %. In this case the model architecture becomes slightly more complex, encompassing 30 trees with a depth of 5. To provide further insights into the classification outcomes, Fig. 8a and b provide a graphical representation of these results, showing the actual and the estimated severity degree for each predicted window. As remarked, the prediction of the model indicates a strong correspondence between the real and predicted system behavior, although the variance and spread of points are higher with respect to the ideal case without turbulence.

Table 5. Metrics computed from the fault detection output considering NTM cases.

Classification report				
Label	Precision	Recall	F1 score	Support
Healthy	0.84	0.89	0.89	24
Misaligned	0.94	0.92	0.99	48

Table 6. Metrics computed from the fault detection and quantification output considering NTM cases.

Classification report				
Label	Precision	Recall	F1 score	Support
Healthy	0.9	0.79	0.78	12
0.5°	1.00	1.00	1.00	11
1.0°	1.00	0.83	0.91	11
1.5°	0.85	1.00	0.86	10
2.0°	0.8	0.91	0.88	14

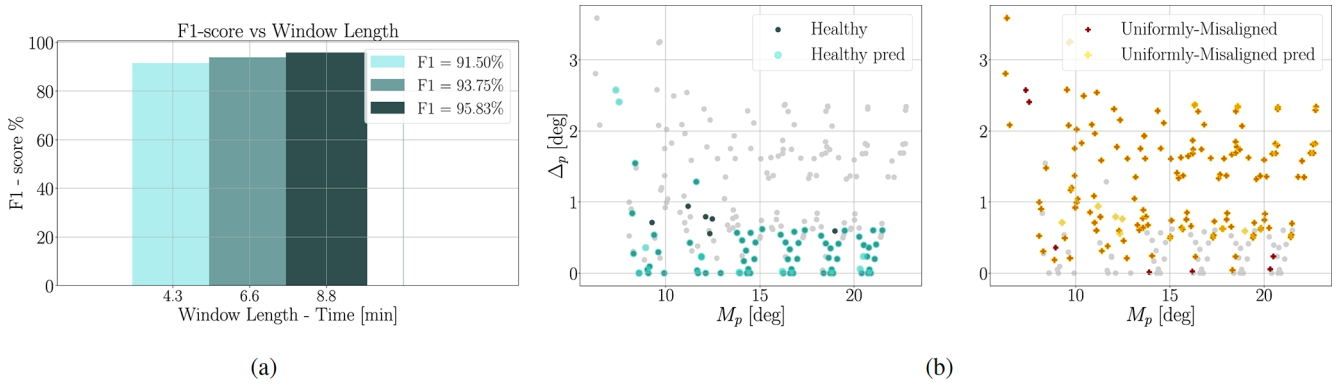

Figure 7. Misalignment detection performance analysis. **(a)** Time window sensitivity analysis showing performance variation with window length. Performance sensitivity to time window length. **(b)** Misalignment detection results: predicted misalignment (lighter colors) compared to actual misalignment (darker colors) across wind speeds. Feature detection consistency across wind speeds.

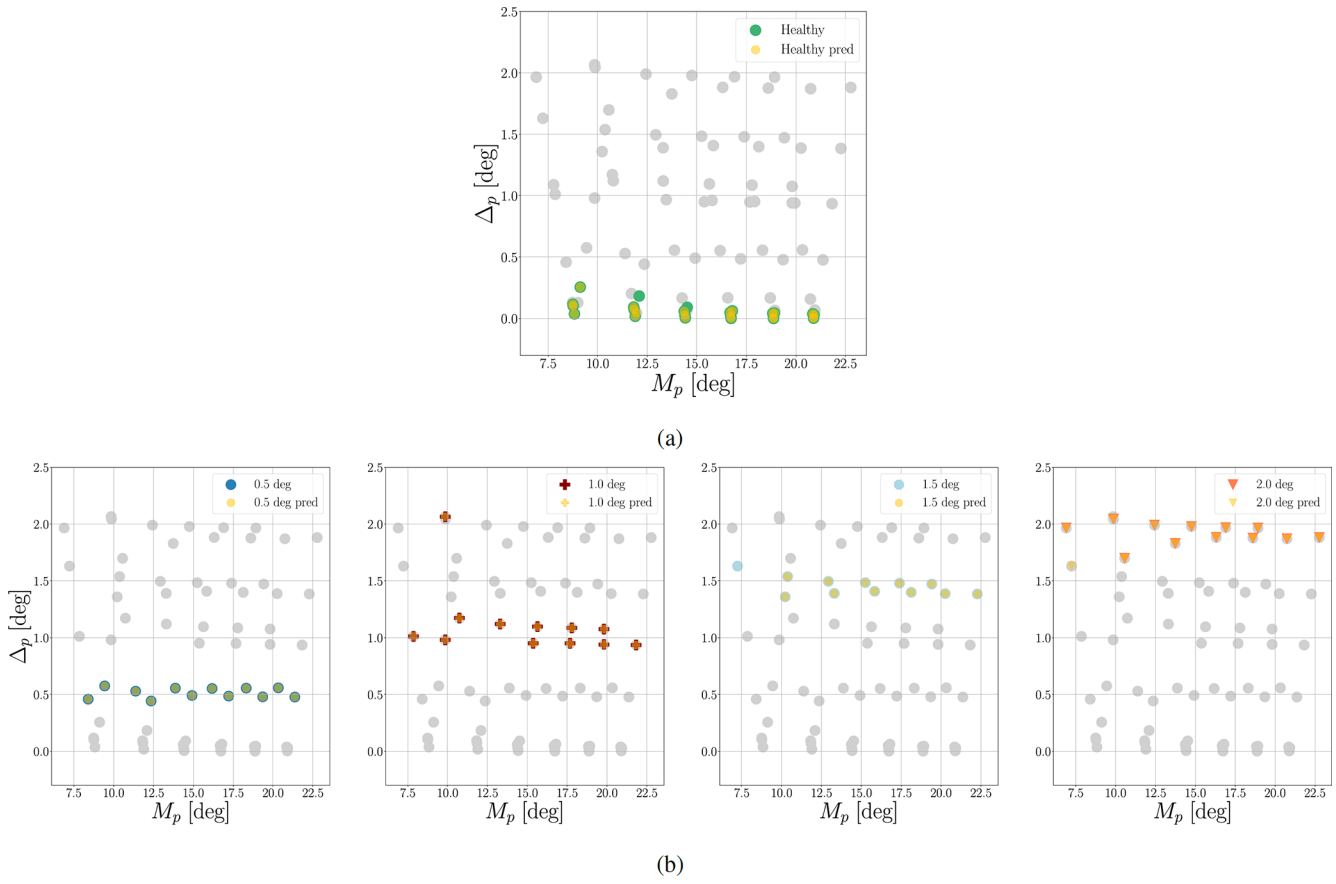

Figure 8. Misalignment severity assessment results for balanced cases in the turbulent wind scenario (NTM). **(a)** Predicted healthy cases. Predicted healthy cases (yellow) compared with actual healthy conditions under turbulent wind scenario. **(b)** Predicted misalignment severity. Predicted misalignment severity (yellow) compared with the actual severity levels under turbulent wind conditions.

4 Conclusions

In this work, we build upon our previously developed machine learning framework method specifically tailored to detecting asymmetrically distributed pitch misalignment in wind turbines. Our goal was to analyze the challenging condition where all the blades are uniformly misaligned by the same degree. In fact, this condition, despite being critical, has been scarcely explored in the literature given its complexity and the overlapping behavior of this case with a healthy

Table 7. Summary of detection and classification performance across all considered scenarios.

Scenario	Power region	Window length	Task	Avg F1 score
NWP	II (5–11 m s^{-1})	4.3 min	Binary detection	99.15 %
NWP	III (13–25 m s^{-1})	4.3 min	Severity classification	97.41 %
NTM	II (5–13 m s^{-1})	10 min	Binary detection	94.1 %
NTM	III (15–25 m s^{-1})	10 min	Severity classification	96.82 %

scenario. Considering the presented results, the proposed approach proves to be robust in both ideal and turbulent wind scenarios and with different wind speeds while preserving its inherent interpretability. Table 7 summarizes the obtained results.

These remarkable results have been achieved by leveraging ad hoc features that are related to the physical behavior of the system. In particular, our strategy extracts time-domain features encompassing the behavior of the required collective pitch demanded of the blades, which we addressed after an accurate sensitivity analysis as the primary indicator of the fault above the rated wind speed. However, for lower wind speeds, we relied on the time-domain behavior of the local mechanical moments on the blades. The mean and standard deviation of these signals and the deviation with respect to a non-anomalous case have been exploited to detect the presence of rotor imbalances and to assess the severity of the misalignment. The validation of this approach has been performed through simulations featuring non-turbulent and turbulent wind conditions, different wind speeds, and different pitch misalignment degrees. This procedure allowed us to assess the performance of the method in detecting and precisely quantifying this anomaly that leads to symmetrical behavior of the system that can mask the fault. More specifically, the method yields an average F1 score of up to 97.41 % in detecting and classifying the anomaly in the case of an ideal scenario of pitch misalignment ranging from 0.5 to 2.0° on all blades, encompassing wind speeds ranging from 5 to 25 m s^{-1}. When considering the more realistic yet noisier scenario of turbulent wind, a longer time frame is required to have optimal performance. Still, the framework achieves an average F1 score of 96.82 % in the detection and quantification of this anomaly, requiring a time window of 10 min.

From a deployment perspective, several practical aspects should be considered. Model training would likely rely on a hybrid strategy combining high-fidelity simulations (digital twin) and SCADA data, since uniformly distributed pitch misalignment events are rare and rarely labeled in field data. Furthermore, a domain shift between simulated and real turbulence, controller tuning, and sensor noise may affect generalization and would require site-specific calibration. In addition, turbulence intensity and wake interactions may increase variability in the collective pitch demand, thus requiring adaptive baselines and potentially longer time windows, as already observed in the NTM scenarios. From an industrial perspective, missed detections (false negatives) are generally more critical, as prolonged operation under uniform misalignment may lead to long-term fatigue damage and efficiency losses. However, excessive false positives should also be avoided to prevent unnecessary inspections and loss of operator trust. Therefore, in practical implementations, threshold tuning should prioritize high recall while maintaining an acceptable false alarm rate. Overall, this work fills a relevant gap in the literature by providing a comprehensive and interpretable solution for the diagnosis of uniformly distributed pitch misalignment, supporting the transition from time-based to condition-based maintenance strategies, with the potential to reduce downtime and improve energy production.

Data availability. The source code, datasets, and related materials cannot be publicly released, as portions of the work are subject to ongoing patent protection and proprietary intellectual property restrictions.

Author contributions. All authors provided fundamental inputs to this work through discussions, feedback, and analyses of the obtained results. S.M., J.L., and M.T. devised the main idea underlining the machine-learning-based detector. S.C. and A.C. identified the physical principles the detector algorithm is anchored on. S.C. and A.C. performed the multibody simulations of the wind turbine in healthy and unhealthy conditions. S.M., J.L., and M.T. implemented and performed the detection strategy.

Competing interests. At least one of the (co-)authors is a member of the editorial board of *Wind Energy Science*. The peer-review process was guided by an independent editor, and the authors also have no other competing interests to declare.

Review statement. This paper was edited by Shawn Sheng and reviewed by two anonymous referees.

References

Al Lahham, E., Kanaan, L., Murad, Z., Khalid, H. M., Hussain, G. A., and Muyeen, S. M.: Online condition monitoring and fault diagnosis in wind turbines: A comprehensive review on structure, failures, health monitoring techniques, and signal processing methods, Energy Rep., 10, 1–23, https://doi.org/10.1016/j.egyr.2024.01.080, 2024.

Bertelè, M., Bottasso, C. L., and Cacciola, S.: Automatic detection and correction of pitch misalignment in wind turbine rotors, Wind Energ. Sci., 3, 791–803, https://doi.org/10.5194/wes-3-791-2018, 2018.

Bodson, M., Chiasson, J., and Novotnak, R. T.: Maximizing wind turbine energy capture using multivariable extremum seeking control, Wind Energy, 17, 589–600, https://doi.org/10.1002/we.1585, 2014.

Bottasso, C. L. and Croce, A.: Cp-Lambda user manual, Tech. Rep., Dipartimento di Scienze e Tecnologie Aerospaziali, Politecnico di Milano, Milano, Italy, 2009–2018.

Breiman, L.: Random forests, Mach. Learn., 45, 5–32, https://doi.org/10.1023/A:1010933404324, 2001.

Cacciola, S. and Riboldi, C. E. D.: Equalizing Aerodynamic Blade Loads Through Individual Pitch Control Via Multiblade Multilag Transformation, J. Sol. Energy Eng., 139, 061008, https://doi.org/10.1115/1.4037744, 2017.

Cacciola, S., Munduate Agud, I., and Bottasso, C. L.: Detection of rotor imbalance, including root cause, severity and location, J. Phys. Conf. Ser., 753, 072003, https://doi.org/10.1088/1742-6596/753/7/072003, 2016.

Cacciola, S., Riboldi, C. E. D., and Croce, A.: Monitoring rotor aerodynamic and mass imbalances through a self-balancing control, J. Phys. Conf. Ser., 1037, 032041, https://doi.org/10.1088/1742-6596/1037/3/032041, 2018.

Ceriani, L. and Verme, P.: The origins of the Gini index: extracts from Variabilità e Mutabilità (1912) by Corrado Gini, J. Econ. Inequal., 10, 421–443, https://doi.org/10.1007/s10888-011-9188-x, 2012.

Dalsgaard, S., Blanke, M., and Brath, P.: Diagnosis of pitch and load effects, International Patent Number WO 2009/059606 A3, US7954372B2, Diagnosis of pitch and load defects, Google Patents, 2009.

Desheng, S., Qian, L., Xin, Z., and Minrong, Z.: Wind turbine variable pitch system fault monitoring method and system, Patent Number CN113586366B, 2021.

IEC requirements book Wind Turbines: Part 1: Design Requirements – DocsLib, Garrad Hassan and Partners Ltd, 3rd Edn., 2004.

Johnson, K. E., Pao, L. Y., Balas, M. J., and Fingersh, L. J.: Experimental evaluation of extremum seeking based region-2 control for a wind turbine, IEEE Trans. Control Syst. Technol., 24, 1084–1091, https://doi.org/10.2514/6.2016-1737, 2016.

Jonkman, J., Butterfield, S., Musial, W., and Scott, G.: Definition of a 5-MW Reference Wind Turbine for Offshore System Development, Tech. Rep. nREL/TP-500-38060, National Renewable Energy Laboratory (NREL), United States, https://www.osti.gov/biblio/947422 (last access: February 2009), 2009.

Krstić, M. and Wang, H.-H.: Stability of extremum seeking feedback for general nonlinear dynamic systems, Automatica, 36, 595–601, https://doi.org/10.1016/S0005-1098(99)00183-1, 2000.

Kusiak, A. and Verma, A.: A Data-Driven Approach for Monitoring Blade Pitch Faults in Wind Turbines, IEEE Trans. Sustain. Energy, 2, 87–96, https://doi.org/10.1109/TSTE.2010.2066585, 2011.

Li, Y. and Wang, J.: Dynamic fault monitoring of wind turbine pitch system using SCADA data, Energies, 12, 3256, https://doi.org/10.3390/en12173256, 2019.

Milani, S., Leoni, J., Cacciola, S., Croce, A., and Tanelli, M.: Automatic Detection and Intensity Classification of Pitch Misalignment of Wind Turbine Blades: a Learning-based Approach, J. Phys. Conf. Ser., 2767, 032010, https://doi.org/10.1088/1742-6596/2767/3/032010, 2024.

Milani, S., Leoni, J., Cacciola, S., Croce, A., and Tanelli, M.: A machine-learning-based approach for active monitoring of blade pitch misalignment in wind turbines, Wind Energ. Sci., 10, 497–510, https://doi.org/10.5194/wes-10-497-2025, 2025.

Qin, S., Tao, J., and Zhao, Z.: Deep learning-based fault diagnosis of wind turbine pitch systems using SCADA data, Energy AI, 14, 100259, https://doi.org/10.1016/j.egyai.2023.100259, 2023.

Rotea, M. A.: Analysis of multivariable extremum seeking algorithms, Automatica, 36, 687–698, https://doi.org/10.1016/S0005-1098(99)00177-6, 2000.

Stetco, A., Dinmohammadi, F., Zhao, X., Robu, V., Flynn, D., Barnes, M., and Keane, J.: Machine learning methods for wind turbine condition monitoring: A review, Renew. Energy, 133, 620–635, https://doi.org/10.1016/j.renene.2018.10.047, 2019.

Tang, B., Song, T., and Deng, L.: Fault detection of wind turbine pitch system based on data-driven methods, Front. Energy Res., 9, 750983, https://doi.org/10.3389/fenrg.2021.750983, 2021.

Tautz-Weinert, J. and Watson, S. J.: Using SCADA data for wind turbine condition monitoring – A review, IET Renew. Power Gener., 11, 382–394, https://doi.org/10.1049/iet-rpg.2016.0248, 2017.

Yang, W., Court, R., and Jiang, J.: Wind turbine condition monitoring by the approach of SCADA data analysis, Renew. Energy, 126, 1–15, https://doi.org/10.1016/j.renene.2018.03.013, 2018.

Zaher, A., McArthur, S. D. J., Infield, D. G., and Patel, Y.: Online wind turbine fault detection through automated SCADA data analysis, Wind Energy, 12, 574–593, https://doi.org/10.1002/we.319, 2009.